NASA TECHNICAL MEMORANDUM

NASA TM X-71760

NASA TM X-71760

MAXIMUM TWO-PHASE FLOW RATES OF SUBCOOLED NITROGEN THROUGH A SHARP-EDGED ORIFICE

by Robert J. Simoneau
Lewis Research Center
Cleveland, Ohio 44135

TECHNICAL PAPER to be presented at
Cryogenic Engineering Conference
Kingston, Ontario, July 22-25, 1975

MAXIMUM TWO-PHASE FLOW RATES OF SUBCOOLED NITROGEN THROUGH A SHARP-EDGED ORIFICE

Robert J. Simoneau

E-8411

ABSTRACT

An experiment was conducted and data are presented in which subcooled liquid nitrogen was discharged through a sharp-edged orifice at flow rates near the maximum. The data covered a range of inlet stagnation pressures from slightly above saturation to twice the thermodynamic critical pressure. The data were taken along five separate inlet stagnation isotherms ranging from 0.75 to 1.035 times the thermodynamic critical temperature.

The results indicate that: (1) subcooled liquids do not choke or approach maximum flow in an asymptotic manner even though the back pressure is well below saturation; (2) orifice flow coefficients are not constant as is frequently assumed. A metastable jet appears to exist which breaks down if the difference between back pressure and saturation pressure is large enough.

INTRODUCTION

The work reported herein is part of a series of experiments (1-5) conducted in recent years at the NASA Lewis Research Center involving two-phase choked flow of liquid cryogens. The essential characteristics of all the experiments were that the initial stagnation conditions were always single-phase and subcooled and that the pressure drop in the flow passage was always to a level below saturation. A wide range of stagnation parameters from well below to above the thermodynamic critical state were examined. The work covered a variety of fluids and geometric openings. The present study deals with a sharp-edged orifice. The general literature on two-phase choked flow has been surveyed in considerable depth by Hsu (6), Henry et al. (7) and Smith (8). As a re-

sult only references which are directly applicable to the present experiment will be discussed herein.

The subject of two-phase flow through orifices is a recurring theme in the literature (9-16). The experiments have been confined to flows of saturated or slightly subcooled liquids, generally at low pressure, except for the work of Hesson and Peck (14), which covered saturated flows over most of the vapor pressure locus of CO_2. The two major points of interest have been whether the flow really chokes and how to predict it. The earlier work (9-13) all concluded that orifices would not choke, while later work (14, 15) claimed to confirm choking. The difference may lie in the loose use of the terms orifice and choking. Frequently, flow passages designated orifices are actually short tubes. Such was the case in references 14 and 15. Uchida and Nariai (16) examined the effect of tube length. They began with a very long tube and kept cutting a little off the inlet until the final run was at an L/D of 1.0. They showed that for short tubes the flow increased as L/D decreased and that, as $L/D \rightarrow 1$, the flow rate of saturated water approached that of cold water. This led them to conclude the saturated water was in a superheated condition which did not vaporize and behaved as single phase water. Uchida and Naviai (16) discharged the flow directly into the atmosphere and did not control back pressure, thus they were not in a position to comment directly on orifice choking; however, they implied no choking in short tubes. Henry (17) summarized some of the work in short tubes and condluded that, for $L/D < 3$, short tube acted as an orifice. It seems from the evidence, especially Bailey (10), that there is a difference in behavior between sharp-edged orifices, short tubes, and long tubes; however, the demarcation between them is not so clear. The orifices of Hesson and Peck (14) and Bonnet (15) were actually short tubes with an $L/D \approx 1.7$. They exhibited choking behavior, (i.e. the flow was unaffected by variations in back pressure). Brennan (13), who like Uchida and Nariai (16) implied no choking, had orifices of L/D from 0.86 to 1.1. The question has practical significance, since in many cases of flow discharge from a vessel it is not possible to control the flow passage geometry.

For reference it is helpful to use gas results since most readers will find them familiar. In this paper the work of Perry (18) will serve this purpose, particularly in the area of the variation of flow with back pressure, (i.e. the question of choking), which will be discussed later.

Attempts at prediction have varied. Authors who concluded the flow would not choke (9, 10, 12, 13, 16) tend to suggest treating the flow as all liquid and recommend the standard equation:

$$G = C_f\sqrt{2\rho_{sat,\,T_o}\,(P_o - P_b)} \qquad (1)$$

Most suggest $C_f = 0.6$ to account for the vena contracta. Richards, et.al. (12) reported the variation of flow coefficient with Reynolds number. Hesson and Peck (14) and Bonnet (15) suggest a two-phase equilibrium calculation and imply a critical throat pressure such as one would expect in nozzles.

The present paper will present a wide range of maximum flow rate data for two-phase flow through a sharp-edged orifice (L/D = 0.19) with subcooled inlet conditions. It will examine the behavior of orifice flow rates as a function of back pressure and will discuss the selection of flow coefficients.

APPARATUS

The test section for this experiment was a sharp-edged orifice as shown in figure 1. Care was taken that the hole edge was sharp and all critical dimensions were carefully measured and are accurate to within ±0.001 cm as shown. Two pressure taps were installed in each of two stations located 1.0 and 4.5 diameters downstream of the orifice entrance as shown in figure 1. The orifice plate was installed between two labyrinth type mixing chambers (4.75 cm I.D.), which took all directionality out of the flow and allowed measurement of inlet, (stagnation), and outlet pressures and temperatures. This assembly was installed in a once-through or blowdown type facility as illustrated in figure 2. The facility is a second generation of the one used in reference (1) and is

described in detail in reference 5. The essential features in the flow sequence are: (1) a pressure vessel; (2) a metering orifice; (3) the test section-mixing chamber assembly; (4) a back pressure control valve; (5) a steam heat exchanger; (6) a second metering orifice. The liquid nitrogen was forced through the system (and the stagnation pressure was set) by application of high pressure ambient gas nitrogen to the top of the liquid in the pressure vessel. The temperature was set by bubbling the same gas in through the bottom of the pressure vessel prior to flow. The test assembly was enclosed in a vacuum chamber to prevent heat loss. Typically it was possible to obtain one or maybe two data points for each sequence of filling and discharge of the pressure vessel. The data were taken along specific stagnation isotherms with stagnation pressures varying anywhere from near saturation to twice the thermodynamic critical pressure.

Pressures were all measured with static strain gage pressure transducers. They had a full scale of 690 N/cm^2 and were rated accurate to within ±0.5 percent by the manufacturer. Before each day's testing the transducers were pressure checked at midspan and throughout the entire experiment they never varied from one another by more than ±0.15 percent. Thus even though the absolute error could be as much as ±3.5 N/cm^2 the relative error between sensors probably never exceeded ±1.0 N/cm^2. Temperatures were measured with platinum resistance thermometers rated accurate to within ±0.1 K. The flow meters were calibrated in a standards laboratory; however, when all the various factors, such as pressure and temperature errors and their effect on density, are considered, it is felt that an error level of ±2 percent must be assigned to the flow measurements. All of the analog data signals were digitized with a scanning digital voltmeter system and transmitted to a central data acquisition and computing facility. It required 15 seconds to acquire all the data and this represented three separate samples of each point. The time factor has a bearing because the experiment, being a blowdown type, is only nominally steady. The pressure vessel typically had a 1 K temperature stratification from top to bottom and thus the stagnation temperature rose steadily throughout the run. A 15 second time slice normally represented a 0.2 K drift in

T_o. The values reported are averages of the three samples.

At the beginning of each day's run a series of checks were run with ambient gas nitrogen, pressurized at about 390 N/cm^2, to insure that the system was operating properly. Over the course of the entire experiment (19 separate checks), the flow rate metered by the downstream orifice was always higher than that by the upstream orifice by between 0 to 1.75 percent, which is well within this measurement tolerance. All of the flow rate data reported herein are based on the upstream meter since it was very close to the test section. The maximum gas flows through the test section as $P_b \rightarrow 0$ were compared to those computed for isentropic equilibrium choked flow of nitrogen through a nozzle using real gas properties. The average ratio of the test orifice to ideal nozzle flow was 0.848 ± 0.003 over the entire course of the experiment. Perry (18) reported 0.84.

ASYMPTOTIC BEHAVIOR OF ORIFICE FLOW RATES

It has long been recognized that a sharp-edged orifice does not choke in the classical understanding of the concept, (i.e. that below a certain pressure further lowering of back pressure will not increase the flow rate). Unfortunately, the literature abounds with references to "choked flow" or "critical flow" orifices. The authors normally mean orifices at or near to their maximum flow rate. This section will examine how a two-phase flow orifice approaches this maximum as the back pressure is decreased.

Ambient Temperature Gas Flows

In order to establish a reference base for the two-phase data it is first necessary to examine the behavior of gas flows. The gas data taken to validate the system and also the work of Perry (18) will be used to form this base. Both the ambient temperature gas and subcooled liquid flow rate data, all at $P_o = 675$ N/cm^2, are shown as a function of back pressure in figure 3. For now attention is restricted to the gas curve (T_o = 275 K). From figure 3 and reference (18) it can be shown that by the

time P_b/P_o decreases to 0.52 (the choking ratio in a nozzle for ambient gas) the orifice flow rate has reached 88 percent of its final value. Two points are important. First, the flow rate increases steadily as the back pressure is reduced toward zero, as expected. Thus, the orifice does not really choke. Second, the approach to the $P_b = 0$ intercept is very gradual and the flow rate appears to approach an asymptotic maximum as P_b decreases towards zero. It is this gradual asymptotic behavior of orifice flow rates that has allowed them to be treated as choked.

Subcooled Liquid Flows

The remaining five isotherms presented in figure 3 are for flows of initially subcooled liquids. Although the 130 K isotherm is above the thermodynamic critical temperature (T_c = 126.3 K), it is grouped with the subcooled liquids because its entropy is less than the thermodynamic critical entropy and in an isentropic expansion it will be on the liquid side of the saturation locus.

Frequently the data points obtained for figure 3 were not exactly on the isotherm or at P_o = 675 N/cm^2, because of the tendency of the system to drift as explained earlier. Thus some data points had to be adjusted to these levels. Adjustments were in the range of 10 N/cm^2 and 2 K. This was done by making special runs to determine the effect of P_o and T_o drift on flow rates at different operating levels. The adjustment coefficients were taken from these results. This may have caused some of the scatter in the data. It should also be pointed out that the pressure discussed here is the system back pressure not the fluid centerline pressure at the minimum area point. Throughout the experiment the pressures at the two downstream measuring stations and in exit plenum were the same to within 1 to 2 N/cm^2.

Looking first at the T_o = 130 K isotherm, which is above T_c = 126.3 K, the flow rate increases more rapidly with decreasing back pressure but it does tend to level off at some asymptotic value. In this case the ratio of the flow rate at $P_b/P_o = 0.52$ to the asymptotic value can be computed from figure 3 to be 0.83, as compared to 0.88 for the ambient gas. The fluid at this temperature level is nor-

mally called a dense gas and, although it expands along the liquid side of the saturation locus, the fluid is quite compressible compared to a liquid.

As the stagnation temperature is lowered below T_c the rate of rise of flow rate with decreasing back pressure continues to increase as is evident in figure 3. The term asymptotic becomes less and less applicable as T_o decreases. The slope is, however, always decreasing as $P_b \rightarrow 0$ and it appears reasonable to project an intercept. In the every case the highest measurable flow rate was within 3 percent of the projected maximum. These curves are similar in shape to those presented by Bailey (10).

Superimposed on the curves of figure 3 is the locus of back pressures which correspond to the isentropic saturation pressure for the given stagnation conditions. These pressures, incidently, are only slightly higher than the throat pressures in a converging-diverging nozzle under the same flow conditions (5). Thus this can also be considered the locus of critical pressures in a choked nozzle. Nothing dramatic happens to the flow rate in the vicinity of this locus to signal a mechanism change. Some insight might possibly be gained from the fluid temperature measurements in the exit plenum. For back pressures above the saturation pressure the exit plenum temperature stayed within ± 0.5 K of the inlet stagnation temperature. One can conclude that the fluid in the exit plenum was probably single phase. Whether any vaporization ever occurred cannot be answered. As back pressures were lowered below the saturation pressure the exit plenum temperature decreased steadily and corresponded to the saturation temperature for the measured back pressure. In this case one would conclude that saturated vapor existed in the exit plenum. Early authors such as Benjamin and Miller (9) and Bailey (10) postulated that no vaporization occurred right at the orifice; but that the flow passes through as a liquid (with a ven contracta) in a metastable state and flashes slightly downstream. This is the basic assumption in the non-equilibrium theory of Henry et. al. (8, 17). The fact that the flow rates in figure 3 did not seem to depend on net downstream quality or the lo-

cation of the saturation pressure would seem to agree with this. This suggests that the test sections of references 14 and 15 were not really orifices but rather tubes ($L/D = 1.7$), and the walls played a role in choking. It would appear for subcooled inlets that, if a free boundary (or jet) exists, two-phase choked flow cannot really occur; however, if the fluid fills the channel before exiting, choking can occur. The choice of $L/D \approx 3$ as a point of demarcation must be reconsidered.

MAXIMUM FLOW RATES

In the present experiment the maximum flow rate through the orifice, G_{max}, will be taken to be that measured at the lowest back pressure attainable in the flow system, which ranged from 19 to 50 N/cm^2 depending on flow conditions, (i.e. two to five times atmospheric pressure). It can be shown from figure 3 that this value for flow rate can be expected to be within 97 percent of the $P_b = 0$ intercept.

The data covered the following range of conditions:

$$95 < T_o < 130 \text{ K}$$

$$80 < P_o < 675 \text{ N/cm}^2$$

$$10 < \left[P_o - P_{sat, S_o}\right] < 620 \text{ N/cm}^2$$

The data are tabulated in Table I. The data were taken along five separate isotherms, four below and one above the thermodynamic critical temperature ($T_c = 126.3$ K). All of the stagnation temperatures presented in Table I are within ± 0.2 K of the particular isotherm. The data tabulation includes the stagnation entropy, and saturation pressures based on stagnation entropy and on stagnation temperature for the convenience of the reader. The back pressures listed in Table I were always at or a little below the saturation pressure corresponding to the exit temperature. This leads to the conclusion that, at the maximum flow rates, there was always vapor in

exit plenum. The maximum flow rate data of Table I are all plotted in figure 4.

FLOW COEFFICIENTS

The normal way to treat flow through orifices is to relate them to an ideal calculation by means of a flow coefficient, such as in equation (1). With respect to the present study two factors require modification of equation (1). First, as the stagnation temperature increases, the density is more sensitive to pressure. Second, the pressure drops across the orifice are very large, as compared to earlier work, and the back pressures are substantially below saturation, somtimes over 200 N/cm^2 below saturation.

The first situation can be handled by using the integral form of equation (1). It can be readily shown (ref. 5) that the basic one-dimensional momentum equation in the absence of friction yields the flow equation in the absence of friction yields the flow equation:

$$G = C_f \left[-2\rho^2 \int_{P_o}^{P_b} \frac{dP}{\rho} \right]^{\frac{1}{2}} \tag{2}$$

In order to use equation (2) a thermodynamic path must be selected. For the pressure from stagnation to saturation an isentropic path seems appropriate. Below the saturation pressure the density is assumed constant at ρ_{sat, S_o}, which is consistent with the metastable assumption. The integrations were carried out for all the data of Table I, using the thermophysical property package GASP (19). The resulting flow coefficients are included in Table I. The flow coefficients are plotted as a function of stagnation pressure in figure 5.

Figure 5 uses P_o as an abscissa rather than the traditional Reynolds number because it is the author's opinion that the peculiar behavior of the flow coefficients in this experiment is phenomenologically related to thermophysical conditions. The Reynolds range is quite high, from 8.2×10^5 to 4.7×10^6, and one would normally expect $C_f = 0.61$ in this range. The Reynolds numbers are in-

cluded in Table I. Figure 5 shows that over most of the 95 K and 110 K isotherms C_f is in fact 0.61. However, for the other isotherms C_f begins at a much lower value, about 0.42, and tends toward 0.61. The average difference between the saturation pressure and the back pressure for the 119, 124, and 130 K isotherms is 177, 225, and 267 N/cm^2, respectively, which is very large. It would appear that because of these very large pressure differences the metastable jet breakdown occurs very near the orifice and interferes with the flow. As P_o increases along an isotherm two things occur which would tend to reduce this interference. First, the difference between saturation and back pressures decreases, typically 50 to 80 N/cm^2 over the P_o range. Second, the driving force, P_c, is increasing. Both of these factors should push the jet further downstream before breaking up and the value of C_f tends toward 0.61, the no interference situation. This same reasoning could account for the slight tailing off at very low P_o along T_o = 95 K. Despite a fairly high pressure difference between saturation and back pressure (95 N/cm^2 average) the 110 K isotherm does not show any such trend. This suggests that the metastable pressure difference which the jet can sustain is very high. The data do not offer detail as to the nature of the interference and thus do not provide an indication for a model to predict this behavior. The data do, however, make it clear that there is a limit to the pressure difference level at which a metastable jet can be sustained without interference with the orifice.

SUMMARY AND CONCLUSIONS

Data have been acquired for maximum two-phase flow rates of subcooled cryogenic nitrogen through a sharp-edged orifice. The initial stagnation conditions were always single-phase and the pressure drop on discharge was to a level substantially below saturation pressure. The data were taken along five stagnation isotherms ranging from 0.75 to 1.03 times the thermodynamic critical temperature. Stagnation pressures ranged from near satura-

tion pressure to twice the thermodynamic critical pressure. The experiment yielded the following conclusions.

1. Subcooled liquids do not choke in a sharp-edged orifice even though the back pressures are well below saturation and two-phase flow clearly exists. The flow rates can be extrapolated an identifiable maximum as back pressure goes to zero. It appears that a metastable liquid jet is maintained through the orifice.

2. Flow coefficients for two-phase maximum flow rates in a sharp-edged orifice are not constant. This suggests that maximum two-phase flow rates cannot be predicted for sharp-edged orifices by simply using some fraction of ideal liquid flow rates. It appears that, if the difference between the saturation pressure and back pressure is large enough, the metastable jet vaporizes close enough to the orifice to interfere with the flow and reduce the flow coefficient.

SYMBOLS

C_f orifice flow coefficient

d orifice diameter, cm

G mass flow rate, gm/cm^2-sec

L/D length to diameter ratio

P pressure, N/cm^2

Re Reynolds number $(Gd/\mu_{sat, S_o})$

S entropy, j/gm-K

T temperature, K

μ dynamic viscosity, gm/cm-sec

ρ density, gm/cm^3

Subscripts

b back or exit plenum conditions

c thermodynamic critical point conditions

o stagnation (inlet) conditions

max maximum value

sat saturation conditions

REFERENCES

1. Hendricks, R. C.; Simoneau, R. J.; Ehlers, R. C.: Choked Flow of Fluid Nitrogen with Emphasis on the Thermodynamic Critical Region. Advances in Cryogenic Engineering, Vol. 18, K. D. Timmerhaus, ed., Plenum Press, 1973, pp. 150-161.

2. Hendricks, R. C.; Simoneau, R. J.; and Hsu, Y. Y.: A Visual Study of Radial Inward Choked Flow of Liquid Nitrogen. Advances in Cryogenic Engineering, Vol. 20, K. D. Timmerhaus, ed., Plenum Press, 1975.

3. Simoneau, R. J.: Two-Phase Choked Flow of Subcooled Nitrogen Through a Slit. Proc. of Tenth Southeastern Seminar on Thermal Sciences, R. C. Watts and H. H. Sogin, eds., Tulane Univ., 1974, pp. 225-238.

4. Hendricks, R. C.; Normalizing Parameters for the Critical Flow Rate of Simple Fluids Through Nozzles. Proc. of Fifth International Cryogenic Engineering Conf., Internl. Inst. Refrigeration, 1974.

5. Simoneau, R. J., Two-Phase Choked Flow of Subcooled Nitrogen in Converging-Diverging Nozzles. NASA TN to be published.

6. Hsu, Yih-Yun: Review of Critical Flow Rate, Propagation of Pressure Pulse, and Sonic Velocity in Two-Phase Media. NASA TN D-6814, 1972.

7. Henry, R. E.; Grolmes, M. A.; and Fauske, H. K.: Pressure Drop and Compressible Flow of Cryogenic Liquid-Vapor Mixtures. Heat Transfer at Low Temperatures, W. Frost, ed., Plenum Press, 1975, pp. 229-259.

8. Smith, R. V.; Randall, K. R.; and Epp, R.: Critical Two Phase Flow for Cryogenic Fluids. (NBS-TN-633, National Bureau of Standards; NASA Order W-13300), NASA CR-130793, 1973.

9. Benjamin, M. W.; and Miller, J. G.: The Flow of Saturated Water Through Throttling Orifices. ASME Trans., vol. 63, No. 5, July 1941, pp. 419-426.

10. Bailey, J. F.; Metastable Flow of Saturated Water. ASME Trans., vol. 73, No. 8, Nov. 1951, pp. 1109-1116.

11. Hoopes, John W.; Flow of Steam-Water Mixtures in a Heated Annulus and Through Orifices. A.I.Ch.E.J. vol. 3, No. 2, June 1957, pp. 268-275.

12. Richards, R. J.; Jacobs, R. B.; and Pestalozzi, W. J.: Measurement of the Flow of Liquefied Gases with Sharp-Edged Orifices. Advances in Cryogenic Engineering. Vol. 4, K. D. Timmerhaus, ed., Plenum Press, 1960, pp. 272-285.

13. Brennan, J. A.: A Preliminary Study of the Orifice Flow Characteristics of Liquid Nitrogen and Liquid Hydrogen Discharging into a Vacuum. Advances in Cryogenic Engineering, Vol. 9, K. D. Timmerhaus, ed., Plenum Press, 1964, pp. 292-303.

14. Hesson, James C.; and Peck, Ralph E; Flow of Two-Phase Carbon Dioxide Through Orifices. A.I.Ch.E.J., vol. 4, No.2, June 1958, pp. 207-210.

15. Bonnet, F. W.; Critical Two-Phase Flow of Nitrogen and Oxygen Through Orifices. Advances in Cryogenic Engineering, Vol. 12, K. K. Timmerhaus, ed., Plenum Press, 1967, pp. 427-437.

16. Uchida, H.; and Nariai, H.: Dishcarge of Saturated Water Through Pipes and Orifices. Proc. of Third Intern. Heat Trans. Conf. Vol. 5, Am. Insti. Chem. Engrs., 1966, pp. 1-12.

17. Henry, Robert E.; The Two-Phase Critical Discharge of Initially Saturated or Subcooled Liquid. Nuc. Sci. Eng., vol. 41, 1970, pp. 336-342.

18. Perry, J. A.: Critical Flow Through Sharp-Edged Orifices. ASME Trans., vol. 71, No. 7, Oct. 1949, pp. 757-764.

19. Hendricks, Robert C.; Baron, Anne K.; and Peller, Ildiko C.: GASP - A Computer Code for Calculating the Thermodynamic and Transport Properties for Ten Fluids: Parahydrogen, Helium, Neon, Methane, Nitrogen, Carbon Monoxide, Oxygen, Fluorine, Argon, and Carbon Dioxide. NASA TN D-7808, 1975.

TABLE I. - DATA SUMMARY - SUBCOOLED NITROGEN FLOW THROUGH A SHARP-EDGED ORIFICE

(a) T_o = 95.1 K.

Rdg	T_o	P_o	T_b	P_b	G_{max}	C_f	$R_e \times 10^{-6}$	S_o	P_{sat, S_o}	P_{sat, T_o}
1239	95.0	80	83.2	19	1710	0.578	0.82	0.837	54	54
1237	95.0	116	84.9	21	2180	.590	1.04	.834	53	54
1304	95.2	147	86.1	24	2520	.600	1.20	.834	53	55
1311	95.2	151	85.8	24	2580	.605	1.23	.833	53	55
1316	95.3	172	86.8	25	2770	.603	1.32	.834	53	55
1253	95.2	198	87.1	27	3000	.605	1.42	.828	52	55
1232	95.0	234	87.6	30	3280	.605	1.53	.820	50	54
1321	95.2	259	87.7	30	3480	.607	1.63	.822	51	55
1233	95.0	291	88.2	31	3760	.614	1.75	.815	49	54
1308	95.3	321	89.3	33	3930	.611	1.83	.817	50	55
1249	95.2	357	89.2	33	4170	.610	1.93	.812	49	55
1245	95.3	394	90.2	36	4420	.616	2.04	.811	49	55
1246	94.9	445	90.7	38	4670	.609	2.12	.798	47	54
1303	95.0	473	90.3	37	4890	.616	2.22	.797	46	54
1235	95.1	499	90.5	37	4990	.611	2.26	.796	46	54
1317	94.9	520	91.0	39	5100	.611	2.30	.790	45	53
1236	95.1	545	91.2	39	5230	.611	2.36	.792	46	54
1274	94.9	576	91.4	40	5370	.609	2.40	.786	45	54
1273	95.1	600	91.5	41	5490	.610	2.46	.789	45	54
1234	95.1	632	91.9	41	5790	.626	2.59	.785	44	54
1272	95.1	672	91.7	41	5870	.614	2.61	.783	44	54

TABLE I. - CONTINUED

(b) T_o = 110.1 K

Rdg	T_o	P_o	T_b	P_b	G_{max}	C_f	$R_e \times 10^{-6}$	S_o	P_{sat, S_o}	P_{sat, T_o}
1037	110.2	168	86.8	26	2540	0.605	1.84	1.170	147	148
1031	109.9	192	87.3	28	2740	.605	1.95	1.158	142	146
1020	110.2	223	87.8	29	2960	.602	2.11	1.159	143	148
1035	110.1	230	88.2	30	3030	.606	2.15	1.156	142	148
1030	110.1	256	88.6	31	3190	.601	2.25	1.150	139	147
1028	110.0	275	89.1	33	3330	.604	2.32	1.143	137	146
1039	110.0	310	89.7	34	3570	.606	2.48	1.139	135	147
1014	109.9	336	90.1	36	3720	.605	2.56	1.132	133	146
1052	110.3	346	90.3	36	3790	.607	2.64	1.137	135	149
1042	110.1	354	90.4	36	3840	.606	2.65	1.133	133	148
991	110.1	364	90.2	36	3900	.606	2.69	1.132	133	148
1054	110.2	407	91.2	39	4140	.607	2.84	1.125	131	148
1041	110.1	417	91.1	38	4200	.606	2.86	1.123	130	148
1055	110.1	439	91.6	40	4320	.608	2.93	1.119	128	148
1008	110.1	460	91.7	40	4420	.606	2.99	1.116	127	148
1053	110.1	460	91.9	41	4460	.611	3.01	1.115	127	147
1018	109.9	464	91.7	41	4430	.604	2.98	1.111	126	146
1045	110.2	489	92.1	42	4570	.607	3.08	1.113	126	148
1017	110.1	493	92.2	42	4580	.605	3.08	1.110	125	147
1062	110.3	555	92.7	44	4890	.607	3.27	1.106	124	150
1064	110.1	575	92.9	44	5000	.608	3.31	1.098	121	148
1061	110.3	585	93.0	44	5040	.607	3.35	1.101	122	149
1007	110.3	599	93.1	45	5100	.607	3.38	1.100	122	149
1046	110.2	623	93.5	46	5220	.608	3.44	1.094	120	148
1006	110.1	632	93.4	47	5240	.606	3.44	1.091	119	148
995	110.2	671	93.5	46	5450	.609	3.56	1.087	117	148

TABLE I. - CONTINUED

(c) T_o = 119.4 K

Rdg	T_o	P_o	T_b	P_b	G_{max}	C_f	$R_e \times 10^{-6}$	S_o	P_{sat, S_o}	P_{sat, T_o}
1137	119.5	251	85.9	25	2100	0.429	2.02	1.402	243	245
1153	119.4	256	86.3	25	2220	.447	2.12	1.395	240	243
1152	119.5	276	87.2	27	2460	.476	2.32	1.388	237	245
1136	119.5	277	87.1	28	2450	.474	2.31	1.389	237	245
1135	119.5	290	87.6	29	2600	.490	2.43	1.382	234	245
1156	119.5	304	88.2	30	2770	.508	2.57	1.375	231	245
1155	119.3	314	88.6	31	2910	.523	2.67	1.367	228	243
1151	119.4	327	89.1	32	3040	.535	2.78	1.363	226	243
1132	119.5	347	89.7	34	3210	.548	2.92	1.359	224	245
1170	119.3	366	90.1	36	3370	.558	3.02	1.347	219	242
1150	119.4	371	90.2	36	3410	.560	3.06	1.348	220	244
1139	119.4	390	90.4	37	3560	.569	3.17	1.342	217	244
1138	119.4	403	90.7	38	3670	.576	3.25	1.337	215	243
1176	119.4	415	91.1	39	3710	.573	3.27	1.334	214	244
1140	119.4	430	91.3	39	3870	.586	3.39	1.328	211	243
1175	119.3	450	91.7	41	3990	.589	3.46	1.322	208	243
1158	119.5	476	92.0	42	4150	.594	3.59	1.319	207	245
1146	119.4	493	92.4	43	4270	.599	3.66	1.312	204	244
1173	119.4	519	92.9	44	4410	.601	3.75	1.306	202	244
1141	119.4	548	93.0	46	4590	.608	3.87	1.299	199	244
1144	119.5	568	93.2	46	4670	.606	3.93	1.297	198	245
1172	119.4	585	93.6	47	4820	.615	4.03	1.291	196	244
1162	119.3	613	93.7	48	4880	.607	4.04	1.283	192	242
1143	119.4	623	93.9	48	4930	.608	4.08	1.284	192	244
1142	119.5	667	94.3	50	5130	.609	4.21	1.276	189	245
1299	119.3	676	94.5	50	5160	.607	4.21	1.270	186	242

TABLE I. - CONTINUED

(d) T_o = 124.4 K

Rdg	T_o	P_o	T_b	P_b	G_{max}	C_f	$R_e \times 10^{-6}$	S_o	P_{sat, S_o}	P_{sat, T_o}
1201	124.4	358	87.5	28	2390	0.426	2.67	1.520	290	312
1200	124.3	375	88.2	30	2600	.450	2.84	1.502	283	311
1199	124.4	388	88.7	31	2740	.465	2.97	1.494	280	312
1185	124.4	392	89.0	32	2780	.469	3.00	1.491	279	312
1183	124.3	416	89.7	34	3040	.494	3.20	1.473	272	310
1224	124.4	418	89.7	34	3020	.490	3.19	1.476	273	312
1187	124.4	426	89.8	35	3100	.497	3.25	1.472	272	312
1198	124.5	430	90.0	35	3130	.500	3.29	1.472	271	313
1186	124.3	441	90.2	36	3240	.508	3.35	1.461	267	311
1197	124.4	455	90.6	37	3360	.518	3.46	1.457	266	312
1210	124.5	461	90.5	37	3390	.504	3.39	1.457	265	313
1209	124.5	473	90.8	37	3500	.528	3.58	1.447	262	312
1208	124.4	483	91.1	39	3620	.536	3.66	1.442	259	312
1207	124.3	503	91.5	39	3740	.543	3.73	1.435	257	311
1189	124.4	517	91.7	41	3820	.547	3.80	1.431	255	312
1188	124.4	547	92.3	42	4030	.558	3.96	1.421	251	312
1230	124.5	553	92.3	43	4060	.560	3.99	1.421	250	313
1191	124.5	570	92.6	43	4160	.563	4.06	1.415	248	313
1192	124.4	575	92.6	44	4210	.567	4.08	1.410	246	311
1194	124.4	587	92.8	44	4310	.573	4.16	1.406	244	311
1190	124.4	595	93.1	45	4350	.574	4.19	1.405	244	312
1202	124.3	611	93.3	46	4500	.584	4.29	1.398	241	311
1203	124.5	629	93.3	46	4540	.581	4.33	1.398	241	313
1205	124.4	647	93.7	47	4690	.590	4.43	1.391	238	312
1228	124.5	677	94.3	49	4810	.590	4.51	1.386	236	314

TABLE I. - CONCLUDED

(e) T_o = 130.1 K

Rdg	T_o	P_o	T_b	P_b	G_{max}	C_f	$R_e \times 10^{-6}$	S_o	P_{sat, S_o}	P_{sat, T_o}
1089	130.1	372	84.2	21	1490	*	*	2.045	312	NA
1088	130.0	375	84.6	22	1540	*	*	2.023	318	
1087	130.2	381	84.7	22	1560	*	*	2.005	322	
1127	130.1	381	84.7	22	1590	*	*	1.993	325	
1076	130.0	401	86.2	25	1870	*	*	1.852	341	
1086	130.1	404	86.1	25	1870	*	*	1.843	341	
1085	130.1	410	86.5	26	1970	0.405	3.61	1.811	342	
1129	130.1	415	86.8	27	2040	.427	3.74	1.784	341	
1114	130.2	431	87.6	28	2220	.415	3.52	1.733	338	
1113	130.0	441	88.0	30	2370	.425	3.49	1.696	334	
1084	130.1	447	88.2	30	2460	.436	3.58	1.668	333	
1126	130.1	454	88.4	31	2510	.437	3.57	1.675	331	
1125	130.0	460	88.7	32	2590	.444	3.59	1.661	329	
1124	130.1	467	89.0	32	2660	.451	3.66	1.655	328	
1082	130.1	480	89.4	33	2790	.461	3.73	1.638	324	
1081	130.1	491	89.6	34	2910	.472	3.82	1.627	322	
1080	130.0	509	90.2	36	3070	.483	3.90	1.605	317	
1079	130.0	526	90.6	37	3220	.495	4.00	1.592	313	
1078	130.0	544	90.9	38	3350	.502	4.08	1.580	309	
1077	130.0	565	91.5	40	3510	.513	4.20	1.565	305	
1103	130.2	588	91.7	41	3660	.523	4.33	1.558	303	
1123	130.0	604	92.1	42	3800	.532	4.41	1.545	298	
1093	130.2	628	92.6	44	3950	.541	4.54	1.538	296	
1120	130.1	645	92.8	45	4050	.544	4.59	1.528	292	
1101	130.2	651	92.9	45	4050	.542	4.59	1.528	292	
1122	130.1	678	93.3	46	4250	.553	4.73	1.515	288	

*Computational scheme described herein not applicable for $S_o > S_c = -1813$.

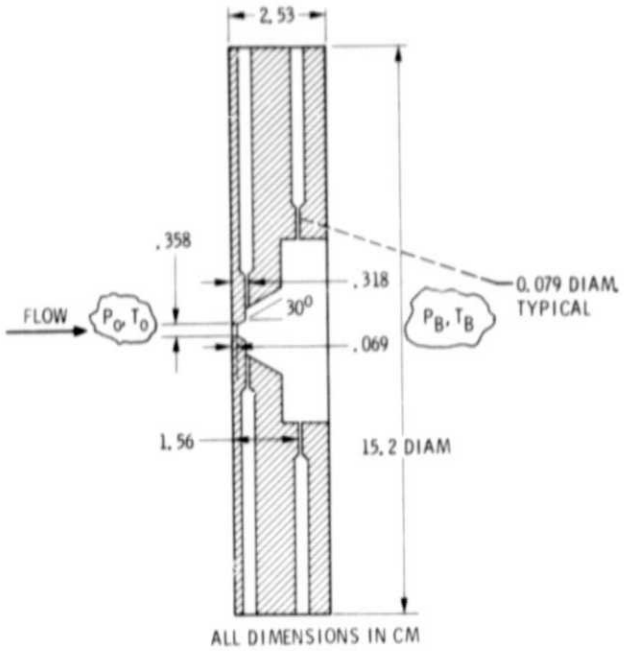

Figure 1. - Sharp edge orifice test section.

E-8411

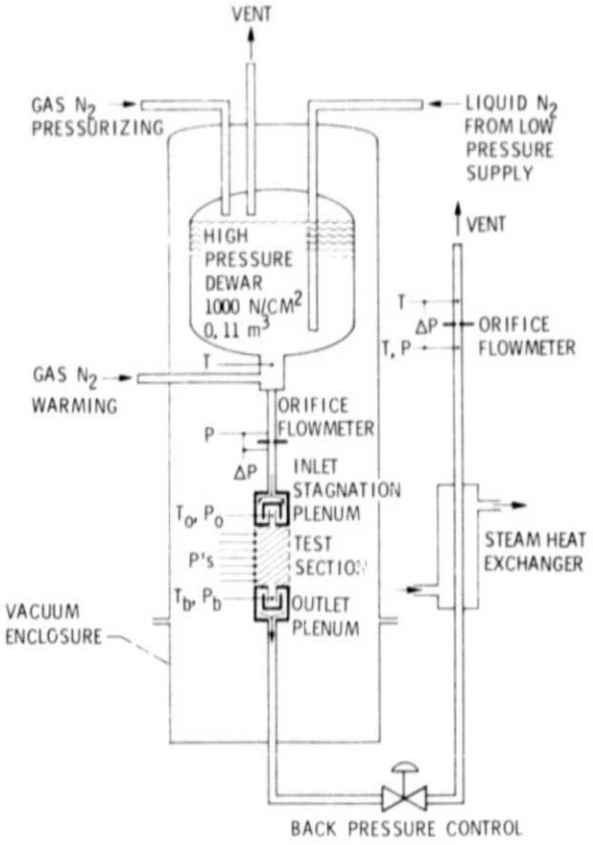

Figure 2. - Flow system schematic.

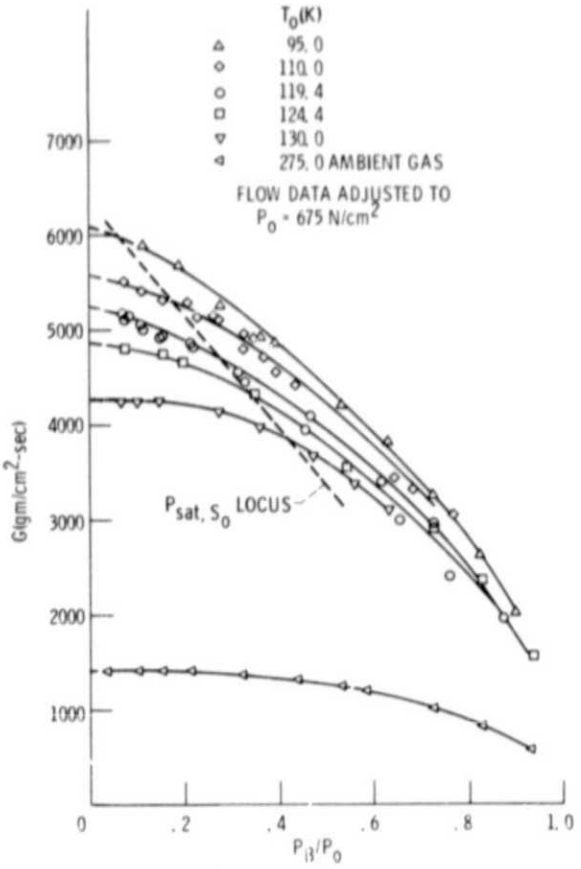

Figure 3. - Variation nitrogen flow rates with back pressure in a sharp-edged orifice.

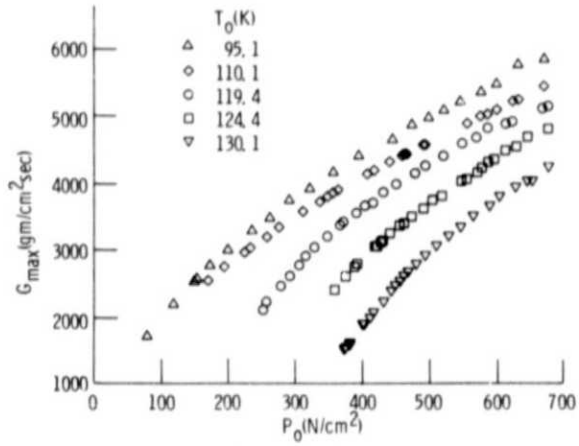

Figure 4. - Maximum flow rates for subcooled nitrogen in a sharp-edged orifice.

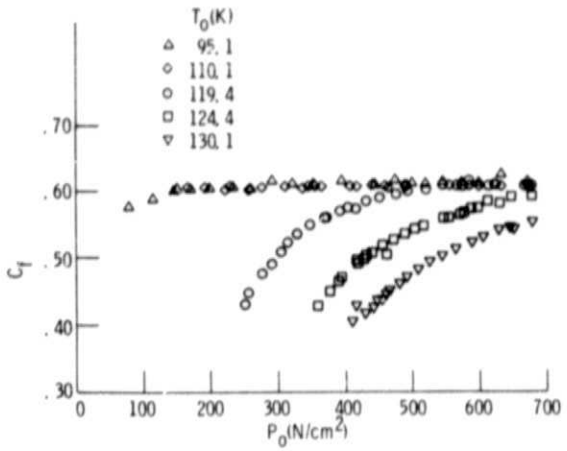

Figure 5. Flow coefficients for a sharp-edged orifice at maximum flow of subcooled nitrogen.